Differentiation of Embryonic Stem Cells to Insulin-Secreting Structures Similar to Pancreatic Islets

Nadya Lumelsky,[1] Olivier Blondel,[1,3] Pascal Laeng,[2,4] Ivan Velasco,[1] Rea Ravin,[1] Ron McKay[1]*

Although the source of embryonic stem (ES) cells presents ethical concerns, their use may lead to many clinical benefits if differentiated cell types can be derived from them and used to assemble functional organs. In pancreas, insulin is produced and secreted by specialized structures, islets of Langerhans. Diabetes, which affects 16 million people in the United States, results from abnormal function of pancreatic islets. We have generated cells expressing insulin and other pancreatic endocrine hormones from mouse ES cells. The cells self-assemble to form three-dimensional clusters similar in topology to normal pancreatic islets where pancreatic cell types are in close association with neurons. Glucose triggers insulin release from these cell clusters by mechanisms similar to those employed in vivo. When injected into diabetic mice, the insulin-producing cells undergo rapid vascularization and maintain a clustered, islet-like organization.

Stem cells are self-renewing elements that can generate the many cell types in the body. They are found in adult and fetal tissues, but the stem cells with the widest developmental potential are derived from an early stage of the mammalian embryo and are named embryonic stem (ES) cells. The isolation of human ES cells and the related embryonic germ (EG) cells has stimulated discussion of the appropriate balance between the clinical benefit and ethical concerns associated with this developing technology (*1*, *2*). ES cells were first obtained in the mouse system where their ability to generate different cell types in vitro has been studied by several groups. This work has defined conditions that promote differentiation of ES cells into cell types found in the blood, heart, muscle, blood vessels, and brain (*3*–*6*). Here we show that the ES cells can be efficiently induced to differentiate into insulin-producing and other cell types typical of endocrine pancreas and that these cells can self-assemble to form functional pancreatic islet-like structures. These results suggest that ES cells will provide a powerful tool to study pancreatic development, function, and disease.

The pancreas is composed of exocrine and endocrine compartments. The endocrine compartment consists of islets of Langerhans, clusters of four cell types that synthesize peptide hormones: insulin (β cells), glucagon (α cells), somatostatin (δ cells), and pancreatic polypeptide (PP cells). The endocrine cells in the islets are organized in a stereotypical topological order and are in close contact with neurons. During embryogenesis, the pancreas develops from a single cell layer of definitive endoderm that contacts the notochord (*7*). Although the adult pancreas and central nervous system (CNS) have distinct origins and functions, similar mechanisms control the development of both organs (*8*–*10*). On the basis of these similarities, we hypothesized that strategies that induce production of neural cells from ES cells could be adapted for endocrine pancreatic cells (*5*, *11*). One of the early steps during neural differentiation of ES cells generates cell populations expressing nestin, an intermediate filament protein normally found in neural precursor cells (*12*). Because nestin has also been recently identified in a subset of immature hormone-negative pancreatic cells (*13*) that, upon differentiation in vitro, give rise to insulin- and glucagon-expressing cells, we examined the expression of endocrine pancreatic genes by the progeny of nestin-positive cell populations derived from ES cells.

Our experimental strategy (*14*) (Fig. 1A) begins with the production of a highly enriched population of nestin-positive cells from embryoid bodies (EBs) (stage 2). A critical step in this strategy is to plate the EBs into a serum-free medium (ITSFn) in which many other cell types die, thus increasing the proportion of nestin-positive cells (*11*) (stage 3). These cells were then expanded in the presence of a mitogen, basic fibroblast growth factor (bFGF), in N2 serum-free medium (*11*) (stage 4), followed by mitogen withdrawal to promote cessation of cell division and differentiation (stage 5). We found that including in the culture media a B27 supplement (*15*) (stages 4 and 5) and nicotinamide (*16*) (stage 5) improved the yield of pancreatic endocrine cells. The outcome of this method is the production of many aggregates of cells expressing insulin.

ES cells at stage 1 express a marker of definitive (embryonic) and visceral (extra-embryonic) endoderm GATA-4 and a marker of definitive endoderm HNF3β. The ES cells at stage 5 also express GATA-4 and HNF3β as well as markers of pancreatic β cell fate, including the murine insulin I, insulin II, islet amyloid polypeptide (IAPP), and the glucose transporter-2 (GLUT 2) (*17*) (Fig. 1B). Glucagon, a marker for the pancreatic α cell, was also induced in differentiated cells. The pancreatic transcription factor PDX-1, which is necessary for pancreatic development (*18*, *19*), was expressed in stage 1 cells. As judged by expression of markers of undifferentiated ES cells alkaline phosphatase and OCT-4 (Fig. 2, A and B) (*20*), the stage 1 cultures are composed predominantly of undifferentiated ES cells. We found that when stage 1 cultures are grown in the absence of feeder cells, they readily express PDX-1. This result indicates that initiation of pancreatic endocrine differentiation takes place early in the development of these ES cell cultures. In fact, expression of PDX-1 has been detected during initial stages of ES cell culture by other investigators (*21*, *22*). Expression of HNF3β, implicated in control of PDX-1 gene expression, as well as visceral endoderm marker GATA-4 have been previously demonstrated to be present during early stages of differentiation of ES cells (*22*). As Fig. 1B shows, PDX-1 expression is down-regulated during differentiation of ES cells. This down-regulation is not surprising, because it is known that PDX-1 mRNA is difficult to detect in the islets of adult rodents (*23*). Overall, the results of reverse transcriptase–polymerase chain reaction (RT-PCR) analysis suggest that these conditions support the differentiation of pancreatic cells from endodermal precursors.

Immunocytochemistry (*24*) was used to identify progenitors, neurons, and insulin-positive cells in the ES cell cultures. Immunoreactivity to nestin was used to detect the differentiating progenitor cells. The intensity of nestin expression increased toward the end of stage 3 (Fig. 1C), and many nestin-positive cells were also present during stage 4. The activation of nestin gene expression coincided with a drastic down-regulation of OCT-4 in stage 3 cells (Fig. 2B). This result shows that efficient conversion of undifferentiated ES cells into nestin-positive progenitors occurs between stages 1 and 3. No insulin-positive cells were detected at stages 1 and 2, but a few cells appeared by the end of stage 3 (Fig. 1C). At the end of stage 4, insulin- and TUJ1-positive (neuron-specific β-III tubu-

[1]Laboratory of Molecular Biology, National Institute of Neurological Disorders and Stroke, National Institutes of Health, [2]Laboratory of System Neuroscience, National Institute of Mental Health, NIH, Bethesda, MD 20892–4092, USA. [3]Human Genome Sciences, Rockville, MD 20850, USA. [4]Psychiatric Genomics, Rockville, MD 20852, USA.

*To whom correspondence should be addressed. E-mail: mckay@codon.nih.gov

lin) (*25*) cells were present (Fig. 1C). Insulin staining continued to increase after mitogen withdrawal, resulting in many strongly insulin-positive cells by the end of stage 5. The number and maturation of neurons also increased during this time, and by the end of stage 5 the majority of insulin-positive cells were localized in tight clusters in close association with neurons (Fig. 1C). We reproducibly observed the same developmental expression pattern in numerous (more than 15) independent experiments and with two different ES cell lines [E14.1 (*26*) and B5 (*27*)].

To estimate the efficiency of generation of insulin-positive cells, we determined the number of insulin-positive cells as a percentage of total cells in the population. Because it is difficult to accurately count the cells in three-dimensional clusters (Fig. 1C and Fig. 3, A through C), we measured the number of insulin-positive cells after dissociation of the cell clusters (*28*, *29*), 31.5 ± 6.6% of which expressed insulin. This number may be somewhat exaggerated because neurons may be preferentially lost during cell dissociation procedure. These results show that this ES cell–based system generates large quantities of insulin-positive cells.

Confocal microscopy was used to analyze the morphology of the cell aggregates. A series of consecutive sections through a cluster shows that insulin-positive cells are located in the interior and are surrounded by neurons [height of the cluster shown (Fig. 3A) is 50 μm and each section is 15 μm thick]. Confocal images failed to detect any TUJ1-insulin double-labeled cells at any developmental stage. To characterize the differentiation further, we performed double immunostaining for insulin and three other pancreatic endocrine hormones: glucagon, somatostatin, and pancreatic polypeptide, which are normally produced by islet cells distinct from insulin-producing cells. We found that all three hormones are generated in the clusters. The majority of glucagon- and somatostatin- positive cells surround the insulin-positive cells (Fig. 3, B and C). We failed to detect expression of the exocrine pancreatic markers amylase and carboxypeptidaseA by RT-PCR or of amylase by immunocytochemistry. The relative distribution of neurons and different types of endocrine cells in the clusters indicates that this system has the ability to generate multicellular structures topographically similar to in vivo pancreatic islets.

The efficient production of islet-like cells and neurons in this system might result from differentiation from two independent progenitors, or from a common progenitor. Clonal analysis was used to distinguish between these two possibilities (*30*). Because ES cells survive poorly when plated at clonal density, we cocultured green fluorescent protein (GFP)–tagged B5 ES cells with the wild-type E14.1 ES cells at stages 4 and 5. This allowed us to obtain individual clones of GFP-labeled cells arising among unlabeled wild-type cells (Fig. 4). Interestingly, in the cytoplasm of GFP-positive cells, the GFP and insulin staining was never co-localized and GFP always surrounded insulin staining (Fig. 4A, inset). A representative clone containing both GFP-positive neurons and β cells is shown in Fig. 4. Of the 50 clones examined in two independent experiments, 44 ± 19.3% contained only neurons ($GFP^+Tuj1^+INS^-$), 18 ± 4.5% contained only insulin-positive cells ($GFP^+Tuj1^-INS^+$), 18 ± 4.5% were not labeled with either insulin or TUJ1 antibody ($GFP^+Tuj1^-INS^-$), and 20 ± 7.6% were labeled with both insulin and TUJ1 antibody ($GFP^+Tuj1^+INS^+$). These results suggest that a common progenitor to neurons and to insulin-positive cells exists in the cell population at the time of initiation of the clonal analysis (beginning of stage 4). In

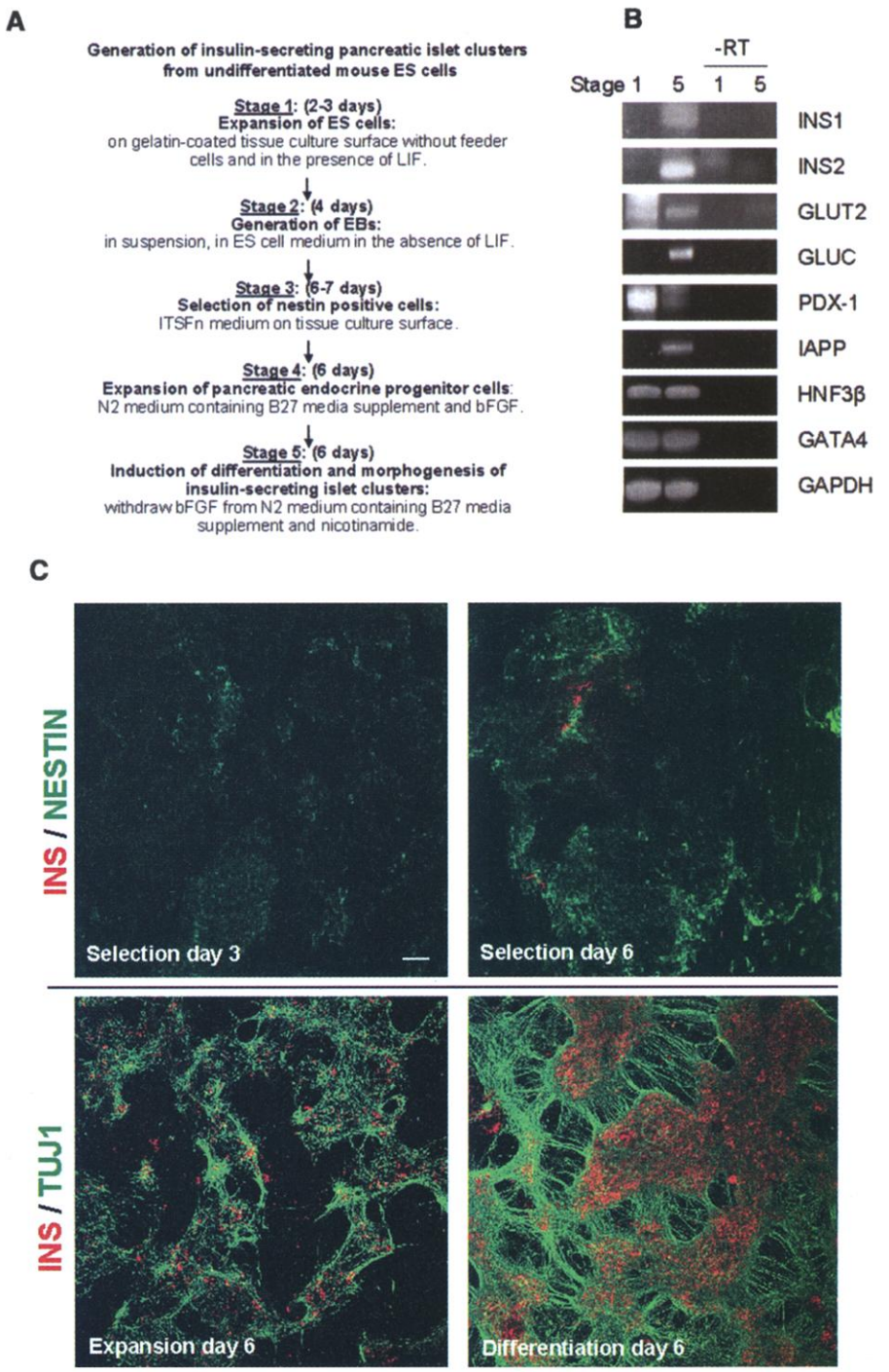

Fig. 1. ES cells generate insulin-positive cells that associate with neurons. (**A**) General outline of the differentiation protocol. (**B**) RT-PCR analysis of pancreatic gene expression by undifferentiated (stage 1) and differentiated (stage 5) E14.1 ES cells. (**C**) Double-immunofluorescence staining for insulin/nestin during and at the end of stage 3, and for insulin–β-III tubulin at the end of stages 4 and 5. Bar, 100 μm.

view of distinct embryonic origins of pancreatic and neural cells, this result may appear surprising. However, the common mechanisms of control and shared nestin expression point to a close relation between pancreatic and neural progenitors. Recent results with stem and progenitor cells of different cell types suggest that, in the future, we may need to re-evaluate and question some of our traditional views on cell lineage relations during differentiation (*31*). This ES cell–based system provides a useful model to further characterize the ontogeny of pancreatic progenitors.

To determine whether insulin-positive cells divide, the proliferating cells were labeled with bromodeoxyuridine (BrdU) at different time points during the culture and then were fixed and immunostained with antibodies to insulin and BrdU (*32*). The peak of cell proliferation coincides with the end of stage 4, but we did not detect BrdU-insulin double-labeled cells at any stage. These results suggest that in this ES cell system, like in vitro cultures of normal pancreatic precursors (*33*), initiation of insulin expression coincides with inhibition of precursor cell proliferation. To determine when insulin expression is initiated, we used a pulse-chase protocol in which cells were first labeled with BrdU and then incubated in the absence of BrdU for different periods of time. Of cells proliferating on day 2 of stage 4, 8.8 ± 2.7% (n = 3 mice) had become insulin-positive by day 6 of stage 4. Of cells proliferating on day 5 of stage 4, 42.2 ± 5.9% (n = 3 cell counting fields) were insulin-positive by day 3 of stage 5. These results establish that a pancreatic precursor was abundant during stage 4, and that a switch from proliferation to differentiation occurs in stage 5.

A series of experiments were conducted to measure glucose-dependent insulin release (*34*). At the end of stage 5, the cells release insulin in response to glucose in a dose-dependent manner with fast kinetics characteristic of primary pancreatic islets in vitro (Fig. 5A) (*35*). Comparison of total cellular insulin content and insulin release at the end of stages 4 and 5 (Table 1) shows that insulin-secreting islet clusters undergo progressive maturation during stage 5. The total insulin content of the cells increased fivefold, and glucose-stimulated insulin release increased more that 40-fold between stages 4 and 5. Assuming that 15% of the cells are insulin-positive (the 15% figure was used to account for preferential death of neurons during cell dissociation), the 145 ng of insulin per milligram of protein translates into 1 μg of insulin per milligram of protein in the insulin-positive subpopulation. Because the

Table 1. ES cells progressively differentiate to store and release insulin. Shown are properties of the cells at the end of the expansion and differentiation stages. Glucose-induced insulin release data correspond to the amount of insulin secreted within 5 min after 20 mM glucose stimulation. Data presented are means ± SEM of the triplicate wells of the same ES cell culture. The results were reproduced in three independent experiments.

	Protein content (mg/well)	Intracellular insulin content (ng/mg protein)	Glucose-induced insulin release (ng/mg protein)	Glucose-induced insulin release (% of insulin content)
6 days of expansion	128 ± 9	28 ± 3	0.07 ± 0.08	0.25 ± 0.27
6 days of differentiation	310 ± 24	145 ± 9	2.87 ± 0.10	1.98 ± 0.07

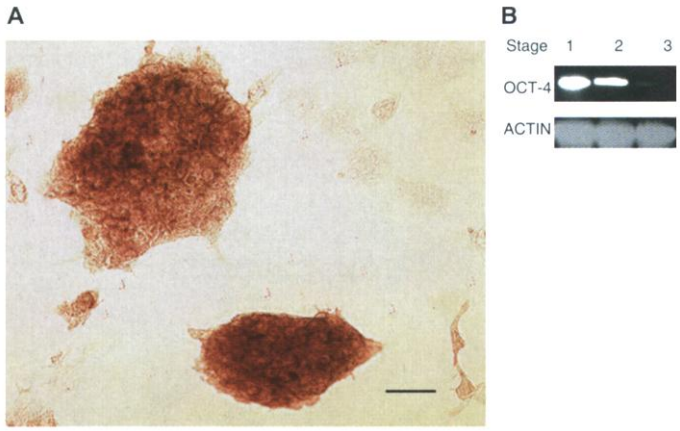

Fig. 2. Stage 1 ES cell populations are composed of undifferentiated ES cells. (**A**) Histochemical staining of stage 1 ES cells for alkaline phosphatase. Bar, 50 μm. (**B**) RT-PCR analysis of expression of a marker of undifferentiated ES cells OCT-4 by undifferentiated E14.1 ES cells (stage 1), EBs (stage 2), and ES cell progeny after selection of nestin-positive progenitors (stage 3).

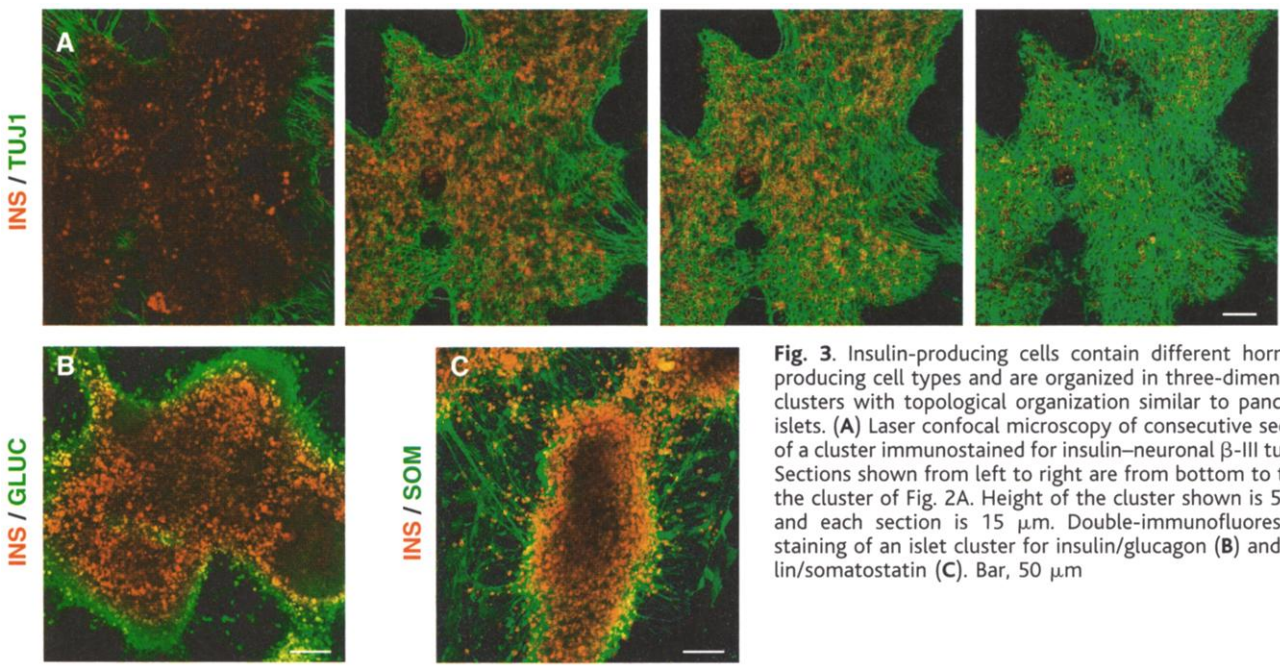

Fig. 3. Insulin-producing cells contain different hormone-producing cell types and are organized in three-dimensional clusters with topological organization similar to pancreatic islets. (**A**) Laser confocal microscopy of consecutive sections of a cluster immunostained for insulin–neuronal β-III tubulin. Sections shown from left to right are from bottom to top of the cluster of Fig. 2A. Height of the cluster shown is 50 μm and each section is 15 μm. Double-immunofluorescence staining of an islet cluster for insulin/glucagon (**B**) and insulin/somatostatin (**C**). Bar, 50 μm

average protein content of a cell is about 20 pg, we conclude that a million insulin-positive cells contains approximately 200 ng of insulin. The insulin content of normal islets is about 10 μg per million cells. Therefore, insulin-positive cells in these cultures contain 50 times less insulin per cell than normal islet cells. These results show that the insulin-positive cells generated in this system produce less insulin than normal pancreatic islet cells. Although the amount of insulin is lower than in normal islets, further studies will likely enhance insulin production. Despite the low insulin production, these data show that insulin secretion occurs in response to physiologically appropriate glucose concentrations.

To determine if the cell clusters use physiological signaling pathways to regulate insulin release, we examined the effect of several agonists and antagonists of insulin secretion. The mechanism by which glucose stimulates insulin secretion in vivo is complex. Transport of glucose into the cell and its metabolism results in adenosine triphosphate (ATP) production, an event which, in turn, leads to inhibition of the ATP-dependent K^+ channels, cell membrane depolarization, opening of the voltage-dependent Ca^{2+} channels, and influx of extracellular Ca^{2+} into the cell (Fig. 5B). Additionally, intracellular Ca^{2+} can be elevated by release of Ca^{2+} from intracellular stores through other mechanisms. Elevation of free intracellular Ca^{2+} is coupled to multiple phosphorylation events modulated by protein kinase C (PKC) and protein kinase A (PKA) cascades, which ultimately lead to release of insulin from the cell (*36*). The results of the effect of the agonists and antagonists on insulin secretion are shown in Fig. 5, C and D. All the agonists tested—a sulfonylurea inhibitor of ATP-dependent K^+ channel (tolbutamide) (*37*), an inhibitor of cyclic-AMP (cAMP) phosphodiesterase [3-isobutil-1-methylxanthine (IBMX)] (*38*), and an agonist of muscarinic cholinergic receptors (carbachol) (*39*)—stimu-

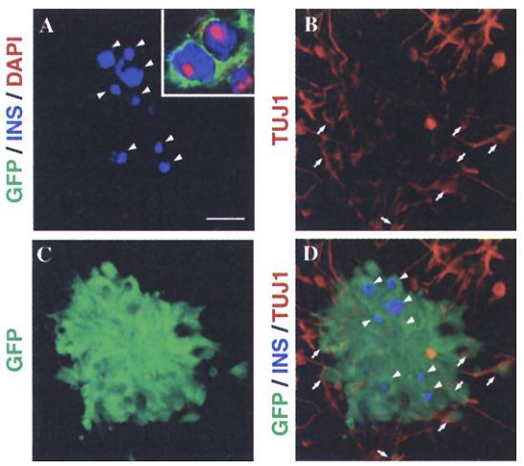

Fig. 4. TUJ1- and insulin-expressing cells can be derived from the same progenitor. (**A** to **D**) show a projection of 20 z section through a GFP-labeled clone derived from a single ES cell. Overlay (D) of the three markers, insulin [(A), in blue], TUJI [(B), in red)], GFP [(C), in green] is shown. GFP$^+$ cells expressing TUJ1 or insulin are shown, respectively, with arrows in (B) and (D) and arrowheads in (A) and (D). Confocal microscopy shows that in B5-GFP$^+$ ES cells grown at clonal density with E14.5 ES cells (A) through (D) or alone at high density [(A), inset], staining for GFP (green) and insulin (blue) within the same cell does not overlap [(A), inset]. Nuclei (DAPI) staining is shown in red. Bar in (A), 20 μm for (A) through (D).

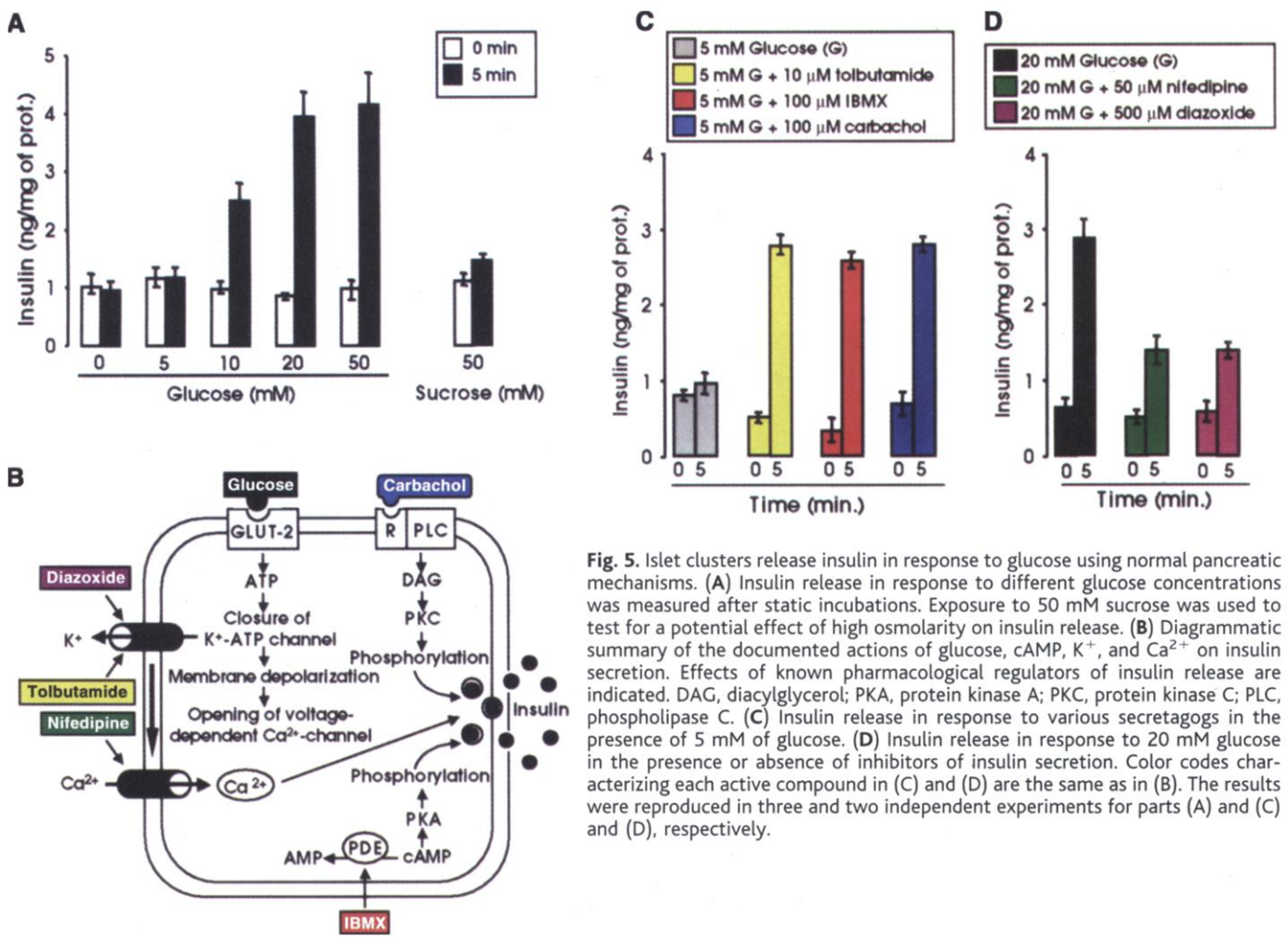

Fig. 5. Islet clusters release insulin in response to glucose using normal pancreatic mechanisms. (**A**) Insulin release in response to different glucose concentrations was measured after static incubations. Exposure to 50 mM sucrose was used to test for a potential effect of high osmolarity on insulin release. (**B**) Diagrammatic summary of the documented actions of glucose, cAMP, K^+, and Ca^{2+} on insulin secretion. Effects of known pharmacological regulators of insulin release are indicated. DAG, diacylglycerol; PKA, protein kinase A; PKC, protein kinase C; PLC, phospholipase C. (**C**) Insulin release in response to various secretagogs in the presence of 5 mM of glucose. (**D**) Insulin release in response to 20 mM glucose in the presence or absence of inhibitors of insulin secretion. Color codes characterizing each active compound in (C) and (D) are the same as in (B). The results were reproduced in three and two independent experiments for parts (A) and (C) and (D), respectively.

lated insulin secretion in the presence of low concentration (5 mM) of glucose. Conversely, the antagonists, diazoxide, an activator of ATP-dependent K^+ channel (*37*), and nifedipine, a blocker of L-type Ca^{2+} channel (one of the Ca^{2+} channels present in β cells) (*40*), inhibited insulin secretion in the presence of high glucose concentrations (20 mM). These results indicate that normal pancreatic machinery is used for glucose-mediated insulin release.

We began testing the potential of ES cell–derived islet-like cell clusters to survive and function in vivo (*41*). For these experiments, stage 5 cell clusters were grafted subcutaneously in the shoulder of streptozotocin-diabetic mice. The blood glucose levels and body weight were monitored at regular intervals. The grafts were harvested and examined after 7 days, 12 days, 4 weeks, and 6 weeks after implantation. The results of analysis of a representative 12-day graft demonstrate that implanted cells vascularize (Fig. 6A) and remain immunoreactive to insulin (Fig. 6B). Moreover, insulin-positive cells form aggregates morphologically similar to normal pancreatic islets (Fig. 6C). We observed analogous cell clustering and insulin immunorectivity in grafts harvested at other times. Although in these experiments we did not observe a sustained correction of hyperglycemia, the grafted animals were able to maintain their body weight and survived for longer periods of time than hyperglycemic sham-grafted controls, suggesting an overall beneficial effect of the grafted cells on the health of the animals. The lack of the diminution of hyperglycemia may not be surprising because the amount of insulin produced by these cells is considerably below that of the native pancreatic islets. Also, a subcutaneous cell implantation might not be ideal for glucose sensing. Nevertheless, these preliminary experiments clearly show the ability of the islet-like clusters to survive and express insulin in vivo.

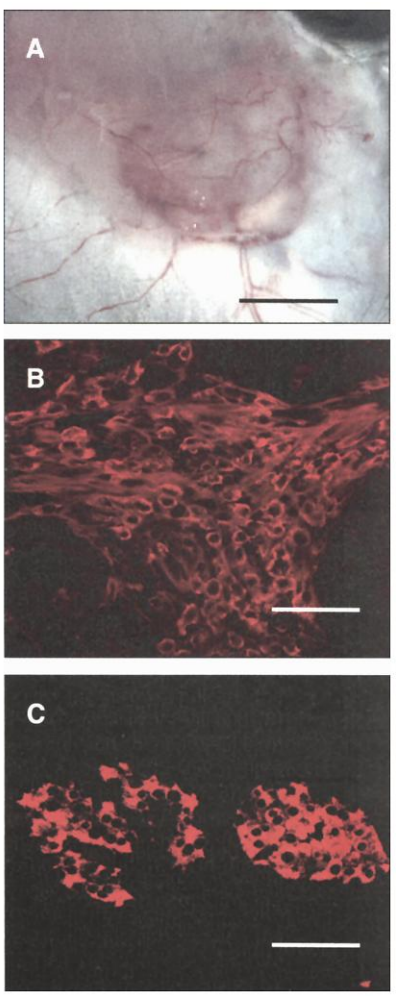

Fig. 6. Stage 5 cells grafted in vivo vascularize and continue to express insulin. (**A**) A graft 12 days after subcutaneous implantation into diabetic mice shows extensive vascularization; see (*41*) for details. Bar, 5 mm. (**B**) Section (20 μm) of the graft shown in (A) immunostained for insulin. (**C**) Section (4 μm) of human pancreas (DAKO) immunostained for insulin. Bar in (B) and (C), 50 μm.

It has been previously demonstrated that ES cells can coordinately differentiate into multiple cell types in vitro (*6*, *11*). We now report that in addition to producing multiple types of pancreatic endocrine cells, this ES cell–based system generates populations that self-assemble into structures resembling pancreatic islets both topologically and functionally. Interestingly, this self-assembling capacity parallels that of the normally dispersed pancreatic endocrine cells that were shown to spontaneously re-associate in vitro into aggregates with three-dimensional architecture typical of native islets (*42*). The results further emphasize how the directed differentiation of ES cells may become a powerful tool to analyze mechanisms controlling the architecture of mammalian organs. It is important to recognize that although more work will be needed to increase insulin production by the cells and to establish various aspects of similarity of these clusters to normal islets, this is the first demonstration of the production of islet-like structures from ES cells. This advance provides an accessible model system to study endocrine progenitor cells, difficult to obtain by existing methods, at multiple stages of development. Another pancreatic ES cell–based system recently described (*43*) uses a gene trap strategy to isolate insulin-secreting cells from ES cells but does not identify the pancreatic progenitor cells that assemble into multicellular structures reported here.

In the clinical context, this ES cell–based system may allow simultaneous generation and assembly of insulin-secreting and other islet cell types known to play important role in regulation of insulin secretion into functional structural units. These units might provide material to optimize insulin production and analyze the fine control of glucose homeostasis. ES cells are ideal for these studies because genetic tools can be used to define the molecular basis of islet development and function. Potential for cell-based therapies is clearly an attractive goal for applications involving human and nonhuman ES and EG cells (*1*, *2*, *11*, *44*). Adult tissue may also be a useful source of functional pancreatic cells (*45*, *46*). The differentiation system described here may provide a source of functional pancreatic islets for treatment of diabetes. To our knowledge, this is the first report showing that the several cell types of endocrine pancreas can be generated from ES cells in vitro. Although pancreatic islets obtained from cadavers can function in the liver after grafting (*47*), issues of tissue rejection and availability remain to be resolved. It is clear that engineering of ES cells to produce an abundant source of immunocompatible tissue for transplantation holds a growing promise for surmounting this and other problems associated with diabetes.

References and Notes

1. J. A. Thomson *et al.*, *Science* **282**, 1145 (1998).
2. M. J. Shamblot *et al.*, *Proc. Natl. Acad. Sci. U.S.A.* **95**, 13726 (1998).
3. G. M. Keller, *Curr. Opin. Cell. Biol.* **7**, 862 (1995).
4. M. G. Klug, M. H. Soonpaa, J. I. Koh, L. J. Field, *J. Clin. Invest.* **98**, 216 (1996).
5. S. Okabe, K. Forsberg-Nilsson, A. C. Spiro, M. Segal, R. D. McKay, *Mech. Dev.* **59**, 89 (1996).
6. J. Yamashita *et al.*, *Nature* **408**, 92 (2000).
7. J. M. Slack, *Development* **121**, 1569 (1995).
8. S. K. Kim, M. Hebrok, D. A. Melton, *Development* **124**, 4243 (1997).
9. H. Li, S. Arber, T. M. Jessell, H. Edlund, *Nature Genet.* **23**, 67 (1999).
10. V. M. Schwitzgebel *et al.*, *Development* **127**, 3533 (2000).
11. S. H. Lee, N. Lumelsky, L. Studer, J. M. Auerbach, R. McKay, *Nature Biotechnol.* **18**, 675 (2000).
12. U. Lendahl, L. B. Zimmerman, R. D. McKay, *Cell* **23**, 585 (1990).
13. H. Zulewski *et al.*, *Diabetes* **50**, 521 (2001).
14. ES cells were cultured as described (*11*) with modifications as follows: B27 media supplement (*15*) (Gibco BRL, Gaithersburg, MA) was added during stages 4 and 5 at final concentration recommended by the manufacturer and nicotinamide (*16*) (Sigma, St. Louis, MO) was added during stage 5 at final concentration 10 mM.
15. G. J. Brewer, J. R. Torricelli, E. K. Evege, P. J. Price, *J. Neurosci. Res.* **35**, 567, (1993)
16. T. Otonkoski, T. M. Beattie, M. I. Mally, C. Ricordi, A. J. Hayek, *J. Clin. Invest.* **92**, 1459 (1993)
17. Total cellular RNA purification and RT-PCR was carried out as previously described (*11*). Identity of the PCR products was confirmed by sequencing. Forward and reverse primer sequences from 5′ to 3′ direction and the length of the amplified products were as follows: insulin I, TAGTGACCAGCTATAATCAGAG and ACGCCAAGGTCTGAAGGTCC (288 bp); insulin II, CCCTGCTGGCCCTGCTCTT and AGGTCTGAAGGTCACCTGCT (212 bp); glucagon, TCATGACGTTTGGCAAGTT and CAGAGGAGAACCCCAGATCA (202 bp); IAPP, GATTCCCTATTTGGATCCCC and CTCTCTGTGGCACTGAACCA (221 bp); Glut2, CCACCCAGTTTACAAGCTC and TGTAGGCAGTACGGGTCCTC (325 bp); PDX-1, TGTAGGCAGTACGGGTCCTC and CCACCCAGTTTACAAGCTC (325 bp); α-amylase-2A, CATTGTTGCACCTTGTCACC and TTCTGCTGCTTTCCCTCATT (300 bp); carboxypeptidase A, GCAAATGTGTGTTTGATGCC and ATGACCAAACTCTTGGACCG (521 bp); GATA-4, CGCCGCCTGTCCGCTTCC and TTGGGCTTCCGTTTTCTGGTTTGA (193 bp); HNF3β, ACCTGAGTCCGAGTCTGACC and GGCACCTTGAGAAAGCAGTC (345 bp); OCT-4, GGCGTTCTCTTTGGAAAGGTGTTC and CTCGAACCACATCCTTCTCT (293 bp); β-actin, ATGGATGACGATATCGCTG and ATGAGGTAGTCTGTCAGGT (568 bp).

18. J. Jonsson, L. Carlsson, T. Edlund, H. Edlund, *Nature* **371**, 606 (1994).
19. M. F. Offield *et al.*, *Development* **122**, 983 (1996).
20. J. Nichols *et al.*, *Cell* **95**, 379 (1998).
21. M. Schuldiner, O. Yanuka, J. Itskovitz-Eldor, D. A. Melton, N. Benvenisty, *Proc. Natl. Acad. Sci. U.S.A.* **97**, 11307 (2000).
22. K. Gerrish *et al.*, *J. Biol. Chem.* **275**, 3485 (2000).
23. D. A. Stoffers, R. S. Heller, C. P. Miller, J. F. Habener, *Endocrinology* **140**, 5374 (1999).
24. Cells were fixed in 4% paraformaldehyde/0.15% picric acid in phosphate-buffered saline (PBS). Immunocytochemistry was carried out with the use of standard protocols. The following primary antibodies were used at following dilutions: nestin rabbit polyclonal 1:500 (made in our laboratory), TUJ1 mouse monoclonal 1:500 and TUJ1 rabbit polyclonal 1:2000 (both from Babco, Richmond, CA), insulin mouse monoclonal 1:1000 (Sigma, St. Louis, MO), insulin guinea pig polyclonal 1:100 (DAKO, Carpinteria, CA), glucagon rabbit polyclonal 1:75 (DAKO), somatostatin rabbit polyclonal 1:100 (DiaSorin, Stillwater, MN), GFP 1:750 polyclonal (Molecular Probes, Eugene, OR), and BRDU rat monoclonal 1:100 (Accurate, antibodies, Westbury, NY). For detection of primary antibodies, fluorescently labeled secondary antibodies (Jackson Immunoresearch Laboratories, West Grove, PA, and Molecular Probes) were used according to methods recommended by the manufacturers. Histochemical staining for alkaline phosphatase cells was carried out using commercially available kit (Sigma) following manufacturer's recommendations.
25. A. Ferreira, A. Caceres, *J. Neurosci. Res.* **32**, 516 (1992).
26. W. W. Kao *et al.*, *Ophthalmol. Vis. Sci.* **37**, 2572 (1996).
27. K. Hadjantonakis, M. Gertsenstein, M. Ikawa, M. Okabe, A. Nagy, *Mech. Dev.* **76**, 79 (1998).
28. For counting of insulin-positive cells, stage 5 ES cell cultures 6 days after bFGF withdrawal were dislodged from tissue culture surface in Ca^{2+}-free 3 mM EDTA containing Krebs-Ringer buffer after incubation for 15 min at 37°C. The clusters were dissociated into single cells, as previously described (*29*). Dissociated cells were allowed to adhere to poly-ornithine/laminine-coated glass coverslips for 5 hours, fixed, immunostained for insulin, and counterstained with a nuclear stain DAPI (4′,6′diamidino-2-phenylindole). This was followed by determination of the percentage of insulin-positive cells in the total cell population.
29. C. B. Wollheim, P. Meda, P. A. Halban, *Methods Enzymol.* **192**, 188 (1990).
30. Stage 3 GFP-labeled B5 ES cells were co-cultured at clonal density on poly-ornithine/fibronectin treated–96-well plates [Costar 3603 (Fisher Scientific, Pittsburgh, PA) black plate with clear and thin bottom] with stage 3 wild-type E14.5 ES cells at a final concentration of 1 B5 cell per 40,000 E14.5 cells per well. B5 cells were plated at a concentration of 1 B5 cell per well using serial dilution. The seeding efficiency and the growth of the plated B5 cells were monitored by immunocytochemical staining for GFP. Two hours after seeding, GFP-positive cells were present in 65 ± 5% of the wells. Counterstaining with a nuclear dye (DAPI) confirmed presence of only one cell per well. After 6 days of differentiation, single GFP-labeled clones derived from a single B5 cell were present in 14.8 ± 1.7% of the wells. Cells were cultured through stages 4 and 5, as shown in Fig. 1A. On day 6 of stage 5, cells were fixed with 4% paraformaldehyde and subjected to triple immunocytochemistry and laser confocal microscopy analysis. For immunocytochemistry, after blocking with a solution of 90% PBS, 10% normal goat serum, and 0.3% Triton-X100, cells were stained with antibodies against insulin [mouse immunoglobulin G1 (IgG1)], GFP (mouse IgG2a), and TUJ1 (rabbit). Cy5, FITC, and Cy3-conjugated goat antibodies to IgG1 mouse, IgG2a mouse and IgG rabbit, respectively, were used as secondary antibodies.
31. S. H. Orkin, *Nature Med.* **6**, 1212 (2000).
32. The cells were labeled with BrdU (Boehringer Mannheim, Indianapolis, IN) at final concentration 10 μm for 24 hours. After the labeling, depending on the specific experiment, the cells were either fixed immediately in 4% paraformaldehyde/0.15% picric acid, treated with 95% ethanol/5% glacial acidic acid for 15 min at room temperature, and subjected to immunocytochemistry, or they were cultured for various lengths of time and then analyzed by immunocytochemistry.
33. A. Vinik, R. Rafaeloff, G. Pittenger, L. Rosenberg, W. Duguid, *Horm. Metab. Res.* **29**, 278 (1997).
34. Insulin secretion was measured using static incubations in Krebs-Ringer with bicarbonate buffer as follows: 120 mM NaCl, 5 mM KCl, 2.5 mM $CaCl_2$, 1.1 mM $MgCl_2$, 25 mM $NaHCO_3$, and 0.1% bovine serum albumin at 37°C. Inhibitors of insulin secretion (nifedipine and diazoxide) were added to the incubation buffer 30 min before addition of glucose. For determination of total cellular insulin content, insulin was extracted from cells with acid ethanol (10% glacial acetic acid in absolute ethanol) overnight at 4°C, followed by cell sonication. Total cellular and secreted insulin was assayed using insulin enzyme-linked immunosorbence assay (ELISA) kit (ALPCO, Windham, NH). Protein concentrations were determined using DC protein assay system (Bio-Rad, Hercules, CA).
35. V. J. Csernus, T. Hammer, D. Peschke, E. Peschke, *Cell. Mol. Life Sci.* **54**, 733 (1998).
36. N. H. McClenaghan, P. R. Flatt, *J. Mol. Med.* **77**, 235 (1999).
37. G. Trube, P. Rorsman, T. Ohno-Shosaku, *Pflugers Arch.* **407**, 493 (1986).
38. W. Montague, J. R. Cook, *Biochem. J.* **122**, 115 (1971).
39. B. Ahren, S. Karlsson, S. Lindskog, *Prog. Brain Res.* **84**, 209 (1990).
40. E. Rojas, J. Hidalgo, P. B. Carroll, M. X. Li, I. Atwater, *FEBS Lett.* **26**, 265 (1990).
41. All animal studies were in accordance with NIH institutional guidelines. Experimental diabetes was induced in 10- to 12-week-old male 129/sv mice (Taconic, Germantown, NY) by a single intraperitoneal injection (150 mg/kg of body weight) of streptozotocin (Sigma) freshly dissolved in 0.1 M of citrate buffer, pH 4.5. Stable hyperglycemia (blood glucose levels 300 to 600 mg/dl) usually developed 48 to 72 hours after the streptozotocin injections. Blood glucose level was determined using Glucometer Elite XL blood glucose meter (Bayer Corp., Elkhart, IN). The animals were grafted with cells or with a buffer vehicle 24 to 48 hours after the establishment of stable hyperglycemia. Injected into each animal were 1 to 2 × 10^7 cells in the form of cluster suspension. In most experiments, day 6 stage 5 cells were used, suspended in Krebs-Ringer–bicarbonate buffer without Ca^{2+}, and injected subcutaneously under isofluorine anesthesia in the shoulder area through a 19-gauge hypodermic needle. To prepare the cluster suspension, the cells cultured on 60-mm tissue culture dishes were carefully dislodged by treatment with Krebs-Ringer–bicarbonate buffer without Ca^{2+} and with 3 mM EDTA for 5 min at 37°C. Each experimental group consisted of five to eight animals per group. The animals were killed at different times, and the grafts were excised and fixed in 4% paraformaldehyde/0.15% picric acid in PBS. Sections of the grafts (15 to 20 μm) were analyzed by immunohistochemistry.
42. P. A. Halban, S. L. Powers, K. L. George, S. Bonner-Weir, *Diabetes* **36**, 783 (1987).
43. B. Soria *et al.*, *Diabetes* **49**, 157 (2000).
44. B. E. Reubinoff, M. F. Pera, C. Y. Fong, A. Trounson, A. Bongso, *Nature Biotechnol.* **18**, 399 (2000).
45. V. K. Ramiya *et al.*, *Nature Med.* **6**, 278 (2000).
46. S. Bonner-Weir *et al.*, *Proc. Natl. Acad. Sci. U.S.A.* **97**, 7999 (2000).
47. A. M. Shapiro *et al.*, *N. Engl. J. Med.* **27**, 230 (2000).

48. We thank T. Doetschman for gift of E14.1 ES cells and A. Nagy for gift of B5 ES cells. We also thank C. Smith for her help with confocal microscopy and J.-H. Kim for alkaline phosphatase analysis of ES cells. I.V. was supported by a fellowship from the PEW charitable Trust. We thank the National Parkinsons Foundation for their support of our work and C. Gerfen for many positive contributions.

8 January 2001; accepted 13 April 2001
Published online 26 April 2001;
10.1126/science.1058866
Include this information when citing this paper.

Autosomal Recessive Hypercholesterolemia Caused by Mutations in a Putative LDL Receptor Adaptor Protein

Christine Kim Garcia,[1] Kenneth Wilund,[1,2] Marcello Arca,[3] Giovanni Zuliani,[4] Renato Fellin,[4] Mario Maioli,[5] Sebastiano Calandra,[6] Stefano Bertolini,[7] Fausto Cossu,[8] Nick Grishin,[9] Robert Barnes,[1] Jonathan C. Cohen,[1] Helen H. Hobbs[1,2*]

Atherogenic low density lipoproteins are cleared from the circulation by hepatic low density lipoprotein receptors (LDLR). Two inherited forms of hypercholesterolemia result from loss of LDLR activity: autosomal dominant familial hypercholesterolemia (FH), caused by mutations in the *LDLR* gene, and autosomal recessive hypercholesterolemia (ARH), of unknown etiology. Here we map the *ARH* locus to a ~1-centimorgan interval on chromosome 1p35 and identify six mutations in a gene encoding a putative adaptor protein (ARH). ARH contains a phosphotyrosine binding (PTB) domain, which in other proteins binds NPXY motifs in the cytoplasmic tails of cell-surface receptors, including the LDLR. ARH appears to have a tissue-specific role in LDLR function, as it is required in liver but not in fibroblasts.

The liver is the major site of synthesis and clearance of cholesteryl ester–rich lipoproteins. More than 70% of circulating LDL is removed from the blood via hepatic LDLR-mediated endocytosis (*1*). In individuals with two mutant LDLR alleles (homozygous FH),